Robust Micro-nanoscale Flowerlike ZnO/Epoxy Resin Superhydrophobic Coating with Rapid Healing Ability

Xin Zhang, Yifan Si, Jiliang Mo, Zhiguang Guo

PII: S1385-8947(16)31576-5
DOI: http://dx.doi.org/10.1016/j.cej.2016.11.014
Reference: CEJ 16015

To appear in: *Chemical Engineering Journal*

Received Date: 31 August 2016
Revised Date: 31 October 2016
Accepted Date: 3 November 2016

Please cite this article as: X. Zhang, Y. Si, J. Mo, Z. Guo, Robust Micro-nanoscale Flowerlike ZnO/Epoxy Resin Superhydrophobic Coating with Rapid Healing Ability, *Chemical Engineering Journal* (2016), doi: http://dx.doi.org/10.1016/j.cej.2016.11.014

Robust Micro-nanoscale Flowerlike ZnO/Epoxy Resin Superhydrophobic Coating with Rapid Healing Ability

Xin Zhang[a], Yifan Si[b,c], Jiliang Mo[a,*], Zhiguang Guo[b,c*]

[a] *Tribology Research Institute, School of Mechanical Engineering, Southwest Jiaotong University, Chengdu, People's Republic of China*

b Hubei Collaborative Innovation Centre for Advanced Organic Chemical Materials and Ministry of Education Key Laboratory for the Green Preparation and Application of Functional Materials, Hubei University, Wuhan 430062, People's Republic of China

[c] *State Key Laboratory of Solid Lubrication, Lanzhou Institute of Chemical Physics, Chinese Academy of Sciences, Lanzhou, People's Republic of China*

Abstract: The development of fabrication techniques for superhydrophobic coatings is rapidly maturing, yet the problem of low mechanical durability still persists. To address this problem, we introduce a robust micro-nanoscale flowerlike ZnO/epoxy resin superhydrophobic coating possessing a rapid healing ability after ultra-abrasion. The coating was fabricated by a simple immersion method, and it presented a water contact angle above 150° and a sliding angle of less than 2°. A simple abrasion test (2400 linear abrasion times at a pressure of 5 kPa) was conducted to show that the coating could maintain superhydrophobicity, even after undergoing thirty abrasion times. Meanwhile, it could be easily repaired within one minute of the coating losing superhydrophobicity under ultra-abrasion. The abrasion only impacted the thickness of the rough structure (grown on the coating surface by immersion) and had almost no effect on the original thickness of the coating itself. This coating had an extremely long service life and may be useful for a wide range of applications.

Keywords: Superhydrophobic; Coating; Micro-nanoscale roughness; Flower-like; Rapid healing ability; Mechanical stability

* Corresponding author. Tel.: 0086-0931-4968105; fax: 0086-0931-8277088. E-mail address: zguo@licp.cas.cn (Guo), jimo@swjtu.cn (Mo)

1. Introduction

The wettability of solid surfaces is a very important property, which is governed by both the chemical composition and the geometrical microstructure of the surface [1-5]. Conventionally, superhydrophobicity is defined as possessing a water contact angle (CA) above 150° and a sliding angle (SA) below 10°. A superhydrophobic surface is produced either by creating a rough surface on a hydrophobic material (CA > 90°) or by modifying a rough surface using materials having a low surface free energy [6-12]. In recent decades, superhydrophobic materials have undergone intense research and have played a key role in addressing a variety of problems. These problems include many industrial and biological applications, such as the deicing and self-cleaning of antennas, windows, automobile windshields, and outdoor textiles, as well as problems requiring enhanced antibacterial and antibiofouling surfaces for medical and marine industries [13-18]. Future applications will include the “free walk on water”, which is the bionic imitation of the microstructure of a water strider’s legs. The feasibility of this application is based on the superhydrophobicity of the water strider’s legs; the maximal force supported by each leg of a water strider is about fifteen times its body weight [19].

The preparation of superhydrophobic surfaces may be performed through a variety of methods, including the sol-gel method [20, 21], the layer-by-layer technique [22, 23], electrochemical etching [24, 25], chemical vapor deposition [26, 27], electrodeposition [28, 29], and wet chemical methods [30] in order to create applications for various needs. The aim is to search for simple and effective methodsfor preparing and controlling the micro-nano structure in order to create a superhydrophobic surface. Peng et al. [20] constructed a superhydrophobic surface on a polydimethylsiloxane substrate via a vapor-liquid sol-gel process with spin coating. Although the surface showed a

good superhydrophobicity with a 162° CA and 2° SA, this method proved to be complicated and expensive. The process occurredin the liquid phase, with the reaction forming a layer of silica particles between the reactant spin-coated on the polydimethylsiloxane surface and the vapor of the acid solution, such that SiO_2 particles could be inlaid on the surface, thereby creating a superhydrophobic surface. To minimize this complexity, it is important to find a simple method to fabricate a superhydrophobic surface. In addition to complexity and high production costs, many practical applications of superhydrophobic surfaces are hampered by poor mechanical durability. For instance, in the study of Li et al. [31], using a simple one-step spray-coating process that sprayed colored stearate particle ethanol suspensions onto stainless steel substrates, a superhydrophobic coating was prepared with a CA larger than 160° and SA less than 5°, prominently demonstrating uniform colors. In addition to its appearance and its good superhydrophobicity, the colorful coating possessed excellent chemical stability under both harsh acidic and alkaline environments. However, a small defect in the coating drastically weakened its mechanical stability such that it could not withstand even simple mechanical friction, like that occurring in the finger test. There are also studies [32-34] regarding the extent of the durability of superhydrophobic surfaces. Chen et al. [32] fabricated a composite coating that possessed excellent superhydrophobicity and robust mechanical durability. After a finger-wipe test, a knife-scratch test, and several cycles with sandpaper, the superhydrophobic coating showed a more robust mechanical durability in comparison to other coatings. Still, in consideration of practical applications, a more desirable coating will be able to recover superhydrophobicity by simple processing, even after losing its superhydrophobicity due to mechanical damage.

For preparing superhydrophobic surfaces, some essential materials with special properties are required. ZnO has uniform particle size, good dispersion, rapid chemical reaction, strong stability, and good adhesion when used as a coating material. Stearic acid (STA) possesses a low surface energy [35-37], while epoxy resin (ER) [38-40] demonstrates good binding capabilities; high mechanical, chemical, and dimensional stability; good corrosion resistance; and easy curing. As such, these materials are commonly used as superhydrophobic materials.

In order to overcome the shortcomings of other coatings, and considering the practical application of superhydrophobic surfaces, we prepared a robust micro-nanoscale flowerlike ZnO/epoxy resin (ZnO/ER) superhydrophobic coating (hereafter referred to as "flowerlike superhydrophobic coating") with rapid healing ability after ultra-abrasion using a simple immersion method [37, 41]. The schematic diagram of the immersion method is shown in Fig. 1. The coating demonstrates a water CA greater than 155° and a SA below 2°. It also possesses excellent mechanical durability: It remains superhydrophobic after thirty abrasion cycles with sandpaper, showing a rapid healing ability, even after ultra-abrasion.

2. Experimental

2.1 Materials

Epoxy resin (E51) and curing agent were purchased from Beijing Oriental Yuhong Waterproof Technology Co., Ltd., China. ZnO (AR) and stearic acid (STA) (CP) were purchased from Shantou Xilong Chemical Plant Co., Ltd., China. Acetic acid and acetone were purchased from Tianjin Lianbohua Pharmaceutical Chemistry Co., Ltd.,

China. All other chemicals were analytical-grade reagents, and were used as received. Millipore water (resistivity ~18 MΩ cm) was used throughout this study.

2.2 Preparation of original ZnO/ER coating

Through a simple mixing method, 8 g of ER and curing agent were mixed at room temperature to form a brown ER solution with a 3:1 mass ratio. Next, white ZnO powders (6 g) were added to the ER solution while stirring. After diluting with 26 mL of acetone solution and stirring for ~30 min at room temperature, a mixture of ZnO/ER was obtained. Finally, the ZnO/ER mixed solution was coated on various solid substrates, such as glass, cloth, and wood. After drying at 80 °C for 5 h, preparation of the original ZnO/ER coating was completed.

2.3 Preparation of micro-nanoscale flowerlike ZnO/ER superhydrophobic coating

The original ZnO/ER coating with substrate was immersed in 20 mL of STA (5 wt%) in order to roughen the surface; then, it was immersed in a 2 M acetic acid/ethanol solution for 0.5 to 7 min in order to reduce the surface free energy [36]. The coating was then dried at ambient conditions for 1 h, thus obtaining the flowerlike ZnO/ER superhydrophobic coating.

2.4 Abrasion test

The abrasion and the abrasion-repaired property of the flowerlike superhydrophobic coating were tested using a rotational sliding abrasion test. This test used sand paper (320 CW) and a standard weight (200 g) to abrade the coating at a pressure of 5 kPa over a distance of 10 cm and at a temperature of ~23 °C.

2.5 Characterization

Field emission scanning electron microscopy (FESEM) images were taken using a JSM-6701F, using Au-sputtered specimens. X-ray photoelectron spectroscopy (XPS)

(ESCALAB 250Xi, Thermo Scientific) measurements were performed using Al-Kα radiation. Fourier transform infrared spectroscopy (FTIR) (Nicolet iS10, Thermo Scientific) recorded the spectra. The water contact angles and the sliding angles were measured (JC2000D) with a 5 μL distilled water droplet at ambient temperature. The CA and SA measurements presented represent averaged values over five different spots on each sample.

3. Results and discussion

3.1 Structure and characterization of micro-nanoscale flowerlike ZnO/ER superhydrophobic coating

The microstructure of the coating was studied by SEM images. Fig. 2a shows the SEM image and CA of the original ER coating, which indicates that the original ER coating surface was smooth and possessed a hydrophilic wettability, demonstrated by a CA of ~36.3°. Superhydrophobic coatings must possess a low surface energy with the materials on the coating surface, as well as the presence of surface roughness. Therefore, a lack of these two conditions led to the hydrophilicity of the original ER coating.

A comparison of Fig. 2a and Fig. 2b clearly shows the ZnO powder on the original ZnO/ER coating surface (Fig. 2b), appearing as white points. The CA (inset in Fig. 2b) indicates that the coating is still hydrophilic, with a CA of ~73.7°. Figs. 2c and 2d show different magnification images of the obtained ZnO/ER superhydrophobic coating. In contrast to the image in Fig. 2b, Fig. 2c shows many microflowers with an average diameter of ~10 μm; every microflower is composed of many nanoscale flakes, as shown in Fig. 2d. The inset of Fig. 2c shows flowerlike superhydrophobic coating having a high water CA, and Fig. S1 (in Supporting Information (SI)) shows the corresponding low SA. Movies S1 and S2 (see SI) further demonstrate that the coating

had a good superhydrophobicity. Fig. S2 (see SI) reveals the formation mechanism of the micro-nanoscale flowerlike structure. It shows that most of the ZnO particles were wrapped in ER on the ZnO/ER coating surface. However, the ER on the coating surface was dissolved by alcohol when the ZnO/ER coating was immersed in STA and acetic acid/ethanol solution, so there are many of these particles exposed on the coating surface. At the same time, the exposed ZnO particles will react with the acetic acid; then, the formation of ZnO particles changes to form micro-nanoscale flowerlike structures. The SEM images only show the roughness of the coating surface, but cannot prove whether the rough surface was modified by STA. Further analysis was performed using XPS (Fig. 3a) and FTIR (Fig. 3b). In Fig. 3, curves 'a' and 'b' represent the ZnO/ER coating and the flowerlike superhydrophobic coating, respectively. As shown in Fig. 3a, the height of the peak of C and the data in the table inset shows that elemental C increased, from 70.1% to 86.9%, indicating that the ZnO/ER coating was modified by the STA. Similarly, Fig. 3b shows the FTIR of the samples. In curve b, the peak at 2921 cm^{-1} is the antisymmetric stretching vibration peak of the C–H bond, and the peak at 2852 cm^{-1} is the symmetric stretching vibration peak of the C–H bond in STA alkyl. The increase of alkyl on the surface further indicates that the ZnO/ER coating was modified by the STA. The XPS and FTIR analyses only prove that STA was absorbed on the coating surface; it doesn't specifically show that STA exists on both the rough topographic and flat surface areas. Perhaps SEM-energy-dispersive X-ray spectroscopy (EDS) can distinguish different elements, but STA and ER both contain the two main elements, C and H, so we suspect that SEM-EDS cannot observe any obvious difference; the STA absorbed on the surface is symmetrical and comprehensive; it exists on both the rough topography area and the flat surface area.

The quantity of ZnO and the immersion time are two major factors in obtaining a superhydrophobic coating. We created six samples using different ZnO amounts and tested the CAs of the samples, as shown in Fig. S3 (see SI). Fig. S3a shows the optical images of the samples with different ZnO amounts. It shows that the samples' surface morphology is appropriate for ZnO amounts of 6, 8, and 10 g. Fig. S3b shows the CAs of the six samples, revealing that the sample with 6 g of ZnO has the best superhydrophobicity. We then produced fifteen samples, obtaining the corresponding CAs after immersion in the mixture for various lengths of time. Fig. 4 shows the wettability of the coating for different immersion times. It can be seen that at least 4 min is necessary to obtain the ZnO/ER superhydrophobic coating. Fig. S4 (see SI) shows the SEM images of the samples for different immersion times, demonstrating that the coating surface will become more wrinkled and rougher for longer immersion times. The reason is that the ER on the surface will slowly dissolve in alcohol; then the wrapped ZnO will become exposed on the surface; the reaction of ZnO and acetic acid eventually will form the rough surface.

The flowerlike superhydrophobic coating in this study could be used on various substrates, due to the good bonding strength and chemical resistance of ER [38]. This expands the practical application of the flowerlike superhydrophobic coating. In addition to the glass substrate used in the earlier analysis, four additional substrates were tested, including fabric, wood, paper, and metal. The left picture of each image in Fig. 5 shows the water droplets on these four substrates. Some of these droplets were absorbed completely, while others existed as an incomplete ball. The right pictures of each image in Fig. 5 show the water droplets on the four substrates with the flowerlike superhydrophobic coating. It shows that all of the droplets exist on the surface as

complete balls of water. The inset figures at the top-left corner of the CA image demonstrate the effectiveness of the superhydrophobicity of the coating on various substrates. Table 1 shows the CA of these four substrates with and without a flowerlike superhydrophobic coating. The left data show the CAs of the original substrates, all of which are below 90°. The right data show the CAs of these four substrates with the flowerlike superhydrophobic coating; all are greater than 153°. As such, all four substrates demonstrate good superhydrophobicity after applying the superhydrophobic ZnO/ER coating created by the method described in this paper. In summary, a comparison of the data in Table 1, the inset pictures of CA, and the shape of the blue water droplets in Fig. 5 all indicate that the flowerlike superhydrophobic coating may be applied to various substrates.

3.2 Chemical durability tests of micro-nanoscale flowerlike ZnO/ER superhydrophobic coating

Real-world applications often require operating under large temperature ranges and in different environments. Therefore, it is necessary to determine the usable temperature range of the flowerlike superhydrophobic coating in this paper. A simple temperature test was arranged. Six samples were prepared and then placed in an oven at several temperatures. Each sample was placed for 1 h in an environment 20 °C higher than the previous sample. Then the CA of the coating was measured after cooling for a few minutes. Fig. 6 shows the data and pictures of the CAs at different temperatures. As shown in this figure, the coating lost superhydrophobicity at 0 °C and 100 °C, while demonstrating superhydrophobicity between 20 °C and 80 °C. It indicates that the ZnO/ER superhydrophobic coating has a wide working temperature range.

Environments differ not only in temperature range, but also others factors. For example, the pH value of rain differs depending on geographic region. A superhydrophobic coating needs to overcome the problems caused by exposure to substances with different pH values. A simple method was used to measure the acid-base resistance property of the flowerlike superhydrophobic coating over a large range of pH values. Fig. 7 clearly shows that the coating lost superhydrophobicity in a strongly alkaline environment, but the change was minimal for lower pH levels. The reason is that the flowerlike superhydrophobic coating was obtained in an acidic solution with the acetic acid and STA, so the STA would exist on the coating surface. Therefore, an acid environment has no impact on the superhydrophobicity of the coating; however, alkaline matter would have a neutralization reaction with the STA on the coating surface, leading to coating loss and, subsequently, loss of superhydrophobicity. The test demonstrated that the flowerlike superhydrophobic coating could adapt to a wide range of pH environments.

3.3 Mechanical stability and durability of micro-nanoscale flowerlike ZnO/ER superhydrophobic coating

Many superhydrophobic coatings have low mechanical stability and durability [31, 42], with even the lightest physical contact damaging the coating. Many studies have investigated ways of increasing the mechanical stability of superhydrophobic coatings [43-47]. For example, Chen et al. [32] fabricated a composite coating that possesses excellent superhydrophobicity and robust mechanical durability, even after undergoing a finger-wipe test, a knife-scratch test, and abrasion with sandpaper. In this paper, a simple abrasion test was performed to quantify the mechanical stability and durability of the flowerlike superhydrophobic coating. As shown in Fig. S5 (see SI), the coating

surface was subjected to a 200-g weight, providing a pressure of 5 kPa while in contact with 320 CW sand paper over a distance of 10 cm.

Water CA measurements were taken after every ten abrasion times. Fig. 8a shows that the CA decreased with the increase of friction cycles. After thirty times, the CA decreased from 160° to 150°， showing that the coating retained its superhydrophobic property. Furthermore, the flowerlike superhydrophobic coating demonstrated an excellent wear-resisting performance. However, the coating lost its superhydrophobic property with the continuous increase in the number of abrasion cycles; however, this does not mean that the coating will fail. Many studies [48-53] have reported that a damaged superhydrophobic surface could recover its superhydrophobicity through a variety of methods. Si et al. [48] create a multifunctional transparent superhydrophobic gel nanocoating with self-healing properties. Bai et al. [49] fabricated a self-recovering superhydrophobic coating that restored superhydrophobicity after immersion in water for several minutes. Li et al. [50] showed that fluorine-free polysiloxane/multiwalled carbon-nanotube surfaces damaged artificially by sand abrasion and water jetting are healable with the help of toluene and curing.

Our abrasion test was continued 2400 times, with the CA determined after every large cycle (every 300 times). The CA of the flowerlike superhydrophobic coating after every cycle was far less than 150°. However, after re-immersion in 20 ml STA (5 wt %) and 2 M acetic acid/ethanol solution, the coating regenerated its superhydrophobicity with a CA of 155 ± 2° (Fig. 8b). Fig. 8b shows the CA before and after friction. Nearly all superhydrophobic coatings have a reusable performance like this (i.e., recovered superhydrophobicity by the original manufacturing method), but they cannot persist for a long time. The flowerlike superhydrophobic coating possessed mechanical durability

and the coating could be repaired many times. The results in Fig. 8b demonstrate that the regenerated superhydrophobic coating could maintain good superhydrophobicity after every large cycle, even after 2400 abrasion times. Fig. 9 shows the comparison of the sectional view before and after friction. It indicates that the thickness of the coating decreased ~37 μm after 2400 abrasion times. As shown in Fig. 9a, the thickness of original ZnO/ER coating was 94 μm, and the raised 37 μm was due to the thickness of the rough surface grown by the chemical reaction of ZnO and acetic acid. The thickness of the coating (~94 μm) after 2400 abrasion times is shown in Fig. 9b. This is nearly equal to the thickness of the original ZnO/ER coating. The result indicates that the 2400 abrasion times just removed the rough surface and had little impact on the ZnO/ER coating. The change of the thickness and abrasion times further confirm that the flowerlike superhydrophobic coating possesses a strong mechanical stability and durability. As such, it is expected to satisfy the requirements for practical applications of a superhydrophobic coating due to easy repairability, as well as strong mechanical stability and durability.

The change in the coating surface was studied by SEM images. Fig. 10 shows the SEM image and the CA of the coating after friction. There are obvious abrasion marks shown in Fig. 10a (the section encircled in red). Figs. 10b and 10c have a higher magnification image than Fig. 10a. In these images, one can see that the coating surface is still rough. The inset in Fig. 10c reveals that superhydrophobicity was lost. The reason is that a superhydrophobic coating needs a combination of rough surface microstructures and low-surface-energy materials. However, friction removed the low-surface-energy material (STA). But re-immersion following the previously described procedure restored the low-surface-energy material, so superhydrophobicity was

recovered, as shown in Figs. 10d–10f. Figs. 10d and 10f show high-magnification images of Fig. 10e. Most of the surface is similar to that seen in Fig. 10f; only a small fraction of the surface has an appearance similar to that in Fig. 10d, the latter of which shows the micro-nanoscale flowerlike structure. Fig. 10f shows the friction-roughened surface with good superhydrophobicity. This is owing to friction roughening the surface and immersion supplying the low-energy material. The micro-nanoscale flowerlike structure is absent after immersion because it needs the chemical reaction of ZnO and acetic acid; as acetic acid was present in the mixed solution, so no ZnO powder was on the coating after friction. It is possible that the ZnO powders were encapsulated by ER, which may explain why they were not exposed to the surface after friction. The problem has not been explained clearly, but it would be an important direction for future study.

The composition was analyzed by XPS and FTIR, as shown in Fig. S6 (see SI). In this figure, elemental C increased from 55.3 % to 76.0 % (Fig. S6a); an increase in the alkyl (Fig. S6b) indicates that the surface was modified by the STA. The coating lost its superhydrophobicity because friction removed the low energy material (STA), but the coating recovered its superhydrophobicity because the analysis showed that the coating was modified by STA after immersion.

3.4 Realistic application of micro-nanoscale flowerlike ZnO/ER superhydrophobic coating

A major goal of scientific materials research is that of practical application; however, most studies have focused on other research aspects. Here, we present some potential practical applications using this new superhydrophobic coating. With the increase in advocacy for environmental protection, more and more paper boxes or bags are being

used to replace plastics. However, paper readily absorbs moisture, decreasing its effectiveness. A 27-cm^3 superhydrophobic box was made using the flowerlike superhydrophobic coating in this study. First, two paper squares with areas of 81 and 36 cm^2, respectively, were prepared (see Fig. 11a). After coating them with ZnO/ER, the papers were immersed in 20 mL STA (5 wt %) and 2 M acetic acid/ethanol solution, and subsequently dried in the ambient environment for 1 h. A superhydrophobic paper box (Fig. 11b) was created by combining these papers, with some powder subsequently placed in the box. Afterwards, a rainy environment was simulated, as shown in Fig. 11c. The box was placed on a water surface for a few minutes, without sinking. Then, water was poured over the surface of the box; the box did not get wet. Additionally, the interior powder was still dry upon opening the box, due to its superhydrophobicity. Movie S3 (see SI) shows this process. A superhydrophobic box possesses many advantages, such as being lightweight, easy to transport, and no pollution, demonstrating just one practical application of the coating in this paper.

4. Conclusions

An immersion method was successfully used to prepare a robust micro-nanoscale flowerlike ZnO/ER superhydrophobic coating with rapid healing ability after ultra-abrasion. The flowerlike superhydrophobic coating showed a water contact angle of 155 ± 2° and a sliding angle of less than 2°, with the rough surface observed in SEM images. A simple abrasion test verified the strong mechanical stability and durability of the coating. When mechanical damage to the coating resulted in the loss of superhydrophobicity, it could be easily repaired with an immersion method and could be re-used many times. The coating offers widespread usage, such as its application on a

variety of substrates, as well as maintaining superhydrophobicity with temperatures ranging from 20 to 80 °C and over a pH range of 1–11. Although the coating has many excellent properties, such as good chemical stability, mechanical durability, and rapid healing ability, improvements may still be made by seeking methods to retain the original state of the substrates and to further standardized materials processing, which will be the subject of future work.

Acknowledgments

This work is supported by the National Nature Science Foundation of China (No. 51522510, No. 51675513, No. 51675448), and the National 973 Project (2013CB632300) for financial support.

References

[1] L. Jiang, Super-hydrophobic nanoscale interface materials: from natural to artificial, Sci. Technol. Rev. 23 (2005) 4-8.

[2] L. Feng, S.H. Li, Y.S. Li, H.J. Li, L.J. Zhang, J. Zhai, Y.L. Song, B.Q. Liu, L. Jiang, D.B. Zhu, Super‐hydrophobic surfaces: from natural to artificial, Adv. Mater. 14 (2002) 1857-1860.

[3] L.P. Wen, Y. Tian, L. Jiang, Bioinspired Super‐Wettability from Fundamental Research to Practical Applications, Angew. Chem. Int. Ed. 54 (2015) 3387-3399.

[4] B. Su, Y. Tian, L. Jiang, Bioinspired interfaces with superwettability: From materials to chemistry, J. Am. Chem. Soc. 138 (2016) 1727-1748.

[5] S. Nishimoto, B. Bhushan, Bioinspired self-cleaning surfaces with superhydrophobicity, superoleophobicity, and superhydrophilicity, Rsc Adv. 3 (2013) 671-690.

[6] M. Ma, R.M. Hill, Superhydrophobic surfaces, Curr. Opin. Colloid Interface Sci. 11 (2006) 193-202.

[7] Y.Y. Yan, N. Gao, W. Barthlott, Mimicking natural superhydrophobic surfaces and grasping the wetting process: A review on recent progress in preparing superhydrophobic surfaces, Adv. Colloid Interface Sci. 169 (2011) 80-105.

[8] B. Wang, Y.B. Zhang, L. Shi, J. Li, Z.G. Guo, Advances in the theory of superhydrophobic surfaces, J. Mater. Chem. 22 (2012) 20112-20127.

[9] E. Celia, T. Darmanin, E.T. de Givenchy, S. Amigoni, F. Guittard, Recent advances in designing superhydrophobic surfaces, J. Colloid Interface Sci. 402 (2013) 1-18.

[10] N.M. Valipour, F.C. Birjandi, J. Sargolzaei, Super-non-wettable surfaces: a review, Colloids Surf., A 448 (2014) 93-106.

[11] Y.F. Si, Z.G. Guo, Superhydrophobic nanocoatings: from materials to fabrications and to applications, Nanoscale 7 (2015) 5922-5946.

[12] Y.P. Tang, X. Xu, H.Z. Cao, Research Progress in Preparation Technology of Micro-Nano Structural Superhydrophobic Materials , Mater. Rev. 11 (2012) 014.

[13] Z.J. Wei, D. Tian, C.L. Xiao, W.L. Liu, Super-hydrophobic surface: From preparation methods to functional application, Chem. Ind. Eng. Prog. 11 (2009) 027.

[14] Q.J. Wang, Q.M. Chen, Recent research advances in manufacturing super hydrophobic membrane and applications, Polym. Mater. Sci. Eng. 2 (2005) 002.

[15] L.L. Cao, A.K. Jones, V.K. Sikka, J.Z. Wu, D. Gao, Anti-icing superhydrophobic coatings, Langmuir 25 (2009) 12444-12448.

[16] Q. Xu, J. Li, J. Tian, J. Zhu, X.F. Gao, Energy-effective frost-free coatings based on superhydrophobic aligned nanocones, ACS Appl. Mater. Interfaces 6 (2014) 8976-8980.

[17] M.J. Nine, M.A. Cole, L. Johnson, D.N. Tran, D. Losic, Robust Superhydrophobic Graphene-Based Composite Coatings with Self-Cleaning and Corrosion Barrier Properties, ACS Appl. Mater. Interfaces 7 (2015) 28482-28493.

[18] J.J. Fu, T. Chen, M.D. Wang, N.W. Yang, S.N. Li, Y. Wang, X.D. Liu, Acid and alkaline dual stimuli-responsive mechanized hollow mesoporous silica nanoparticles as smart nanocontainers for intelligent anticorrosion coatings, ACS nano. 7 (2013) 11397-11408.

[19] X.F. Gao, L. Jiang, Recent studies of natural superhydophobic bio-surfaces, PHYSICS-BEIJING-. 35 (2006) 559.

[20] Y.T. Peng, K.F. Lo, Y.J. Juang, Constructing a Superhydrophobic Surface on Polydimethylsiloxane via Spin Coating and Vapor-Liquid Sol-Gel Process, Langmuir 26 (2009) 5167-5171.

[21] B. Dyett, R. Lamb, Correlating Material Properties with the Wear Behavior of Sol-Gel Derived Superhydrophobic Films, Adv. Mater. Interfaces (2016) DOI: 10.1002/admi.201500680.

[22] L.B. Zhang, H. Chen, J.Q. Sun, J.C. Shen, Layer-by-layer deposition of poly (diallyldimethylammonium chloride) and sodium silicate multilayers on silica-sphere-coated substrate-facile method to prepare a superhydrophobic surface, Chem. Mater. 19 (2007) 948-953.

[23] Y.M. Yang, Fabrication of Antireflective Self-Cleaning Surfaces Using Layer-by-Layer Assembly Techniques, Self-Cleaning Materials and Surfaces: A Nanotechnology Approach (2013) 277-311.

[24] Y. Lu, J.L. Song, X. Liu, W.J. Xu, Y.J. Xing, Z.F. Wei, Preparation of superoleophobic and superhydrophobic titanium surfaces via an environmentally

friendly electrochemical etching method, ACS Sustainable Chemistry & Engineering 1 (2012) 102-109.

[25] T. Darmanin, E.T.d. Givenchy, S. Amigoni, F. Guittard, Superhydrophobic surfaces by electrochemical processes, Adv. Mater. 25 (2013) 1378-1394.

[26] H. Liu, L. Feng, J. Zhai, L. Jiang, D.B. Zhu, Reversible wettability of a chemical vapor deposition prepared ZnO film between superhydrophobicity and superhydrophilicity, Langmuir 20 (2004) 5659-5661.

[27] Z.M. Shen, C.C. Hou, S.S. Liu, Z.S. Guan, Micro-nanostructured silicone-carbon composite coatings with superhydrophobicity and photoluminescence prepared by oxidative chemical vapor deposition, J. Appl. Polym. Sci. 131 (2014) 40400-40409.

[28] Q. Liu, D.X. Chen, Z.X. Kang, One-step electrodeposition process to fabricate corrosion-resistant superhydrophobic surface on magnesium alloy, ACS Appl. Mater. Interfaces 7 (2015) 1859-1867.

[29] L.Y. Xu, S.S. Chen, X.M. Lu, Q.H. Lu, Electrochemically Tunable Cell Adsorption on a Transparent and Adhesion-Switchable Superhydrophobic Polythiophene Film, Macromol. Rapid Commun. 36 (2015) 1205-1210.

[30] Y.Y. Sun, M. Chen, S.X. Zhou, J. Hu, L.M. Wu, Controllable Synthesis and Surface Wettability of Flower-Shaped Silver Nanocube-Organosilica Hybrid Colloidal Nanoparticles, ACS nano. 9 (2015) 12513-12520.

[31] J. Li, R.N. Wu, Z.J. Jing, L. Yan, F. Zha, Z.Q. Lei, One-step spray-coating process for the fabrication of colorful superhydrophobic coatings with excellent corrosion resistance, Langmuir 31 (2015) 10702-10707.

[32] L. Chen, X.Y. Sun, J.Z. Hang, L.J. Jin, D. Shang, L.Y. Shi, Large-Scale Fabrication of Robust Superhydrophobic Coatings with High Rigidity and Good Flexibility, Adv. Mater. Interfaces (2016) DOI: 10.1002/admi.201500718.

[33] C.D. Ding, Y. Liu, M.D. Wang, T. Wang, J.J. Fu, Self-healing, superhydrophobic coating based on mechanized silica nanoparticles for reliable protection of magnesium alloys, Journal of Materials Chemistry A. 4 (2016) 8041-8052.

[34] X.F. Ding, S.X. Zhou, G.X. Gu, L.M. Wu, A facile and large-area fabrication method of superhydrophobic self-cleaning fluorinated polysiloxane/TiO 2 nanocomposite coatings with long-term durability, Journal of Materials Chemistry. 21 (2011) 6161-6164.

[35] Y.Q. Qing, Y. Zheng, Y. He, C.B. Hu, Q. Mo, Preparation and Properties of ZnO/Polydimethylsiloxane Superhydrophobic Films, China Plast. Ind. 7 (2013) 034.

[36] F.W.H. Kruger, W.J. McGill, A DSC study of curative interactions. I. The interaction of ZnO, sulfur, and stearic acid, J. Appl. Polym. Sci. 42 (1991) 2643-2649.

[37] C.Q. Wang, J.Y. Xiao, J.C. Zeng, D.Z. Jiang, Z.Q. Yuan, A novel method to prepare a microflower-like superhydrophobic epoxy resin surface, Mater. Chem. Phys. 135 (2012) 10-15.

[38] H.B. Gu, C. Ma, J.W. Gu, J. Guo, X.R. Yan, J.N. Huang, Q.Y. Zhang, Z.H. Guo, An overview of multifunctional epoxy nanocomposites, J. Mater. Chem. C. 4 (2016) 5890-5906.

[39] H. Pan, G. Sun, T. Zhao, G.H. Wang, Thermal properties of epoxy resins crosslinked by an aminated lignin, Polym. Eng. Sci. 55 (2015) 924-932.

[40] Y.F. Si, Z.G. Guo, W.M. Liu, A Robust Epoxy Resins@ Stearic Acid-Mg $(OH)_2$ Micro-nanosheet Superhydrophobic Omnipotent Protective Coating for Real Life Applications, ACS Appl. Mater. Interfaces. 8 (2016) 16511-16520.

[41] Y. Wang, X.W. Liu, H.F. Zhang, Z.P. Zhou, Superhydrophobic surfaces created by a one-step solution-immersion process and their drag-reduction effect on water, RSC Adv. 5 (2015) 18909-18914.

[42] W.H. Xu, L.D. Zhang, L. Zhao, S.H. Chen, L. Wang, W.L. Liu, Research progress on the durability of super hydrophobic surface, Chem. Eng. Prog. 31 (2012) 2260-2264.

[43] N. Yokoi, K. Manabe, M. Tenjimbayashi, S. Shiratori, Optically transparent superhydrophobic surfaces with enhanced mechanical abrasion resistance enabled by mesh structure, ACS Appl. Mater. Interfaces 7 (2015) 4809-4816.

[44] I. Das, G. De, Zirconia based superhydrophobic coatings on cotton fabrics exhibiting excellent durability for versatile use, Sci. Rep. 5 (2015) 18503-18514.

[45] V. Kondrashov, J. Rühe, Microcones and nanograss: toward mechanically robust superhydrophobic surfaces, Langmuir 30 (2014) 4342-4350.

[46] L.B. Boinovich, A.M. Emelyanenko, V.K. Ivanov, A.S. Pashinin, Durable icephobic coating for stainless steel, ACS Appl. Mater. Interfaces 5 (2013) 2549-2554.

[47] A. Milionis, E. Loth, I.S. Bayer, Recent advances in the mechanical durability of superhydrophobic materials, Advances Colloid Interface Sci. 229 (2016) 57-79.

[48] Y.F. Si, H. Zhu, L.W. Chen, T. Jiang, Z.G. Guo, A multifunctional transparent superhydrophobic gel nanocoating with self-healing properties, Chem. Commun 51 (2015) 16794-16797.

[49] N.N. Bai, Q. Li, H.Z. Dong, C. Tan, L. Xu, A versatile approach for preparing self-recovering superhydrophobic coatings, Chem. Eng. J. 293 (2016) 75-81.

[50] B.C. Li, J.P. Zhang, Polysiloxane/multiwalled carbon nanotubes nanocomposites and their applications as ultrastable, healable and superhydrophobic coatings, Carbon 93 (2015) 648-658.

[51] Y. Liang, M.D. Wang, C. Wang, J. Feng, J.S. Li, L.J. Wang, J.J. Fu, Facile Synthesis of Smart Nanocontainers as Key Components for Construction of Self-Healing Coating with Superhydrophobic Surfaces, Nanoscale research letters. 11 (2016) 231.

[52] K.L. Chen, S.X. Zhou, L.M. Wu, Fabrication of All‐Water‐Based Self‐Repairing Superhydrophobic Coatings Based on UV‐Responsive Microcapsules, Advanced Functional Materials. 25 (2015) 1035-1041.

[53] K.L. Chen, S.X. Zhou, L.M. Wu, Self-Healing Underwater Superoleophobic and Antibiofouling Coatings Based on the Assembly of Hierarchical Microgel Spheres, ACS nano. 2015, 10 1386-1394.

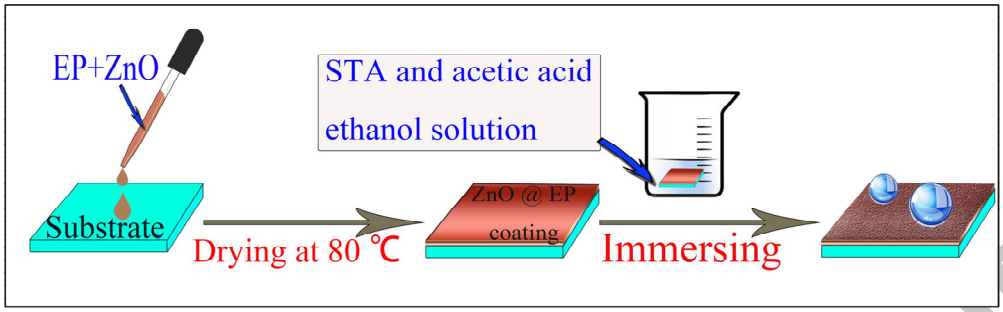

Fig.1 Schematic illustrating the production process of the micro-nanoscale flowerlike ZnO/ER superhydrophobic coating.

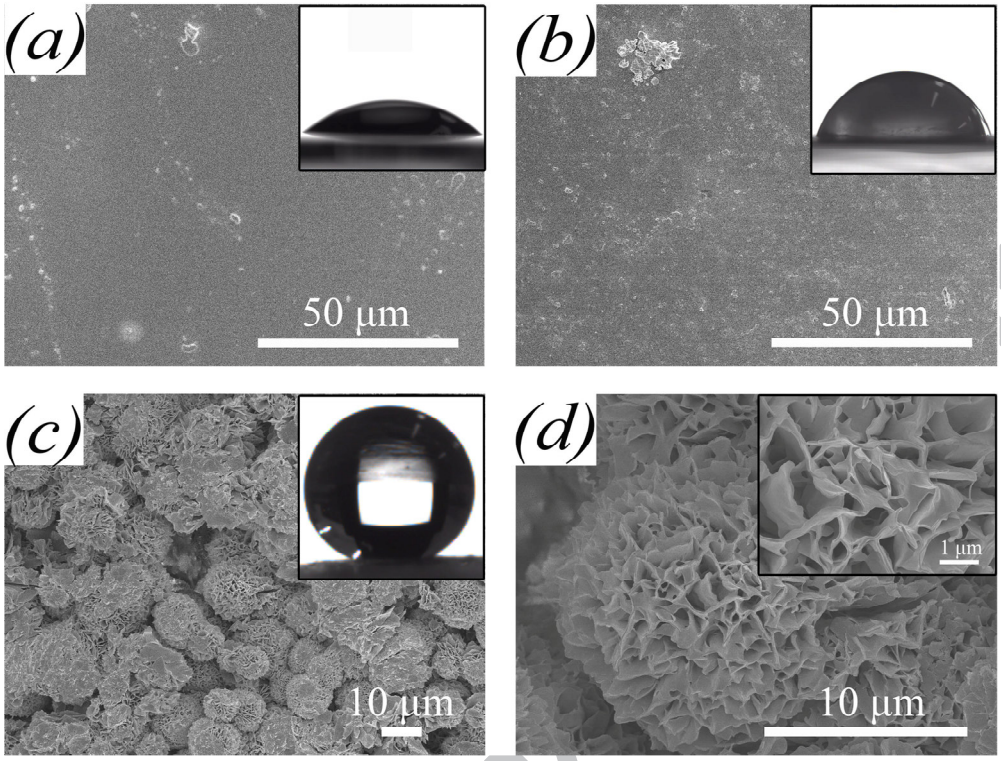

Fig. 2 SEM images of original ER coating (a), ZnO/ER coating (b), and low-(c) and high-(d) magnification images of micro-nanoscale flowerlike ZnO/ER superhydrophobic coating. Shown in the insets of (a), (b), and (c) are the optical images of static water droplets (5 μL). Inset (d) is the greater magnification SEM image taken from micro-nanoscale flowerlike ZnO/ER superhydrophobic coating.

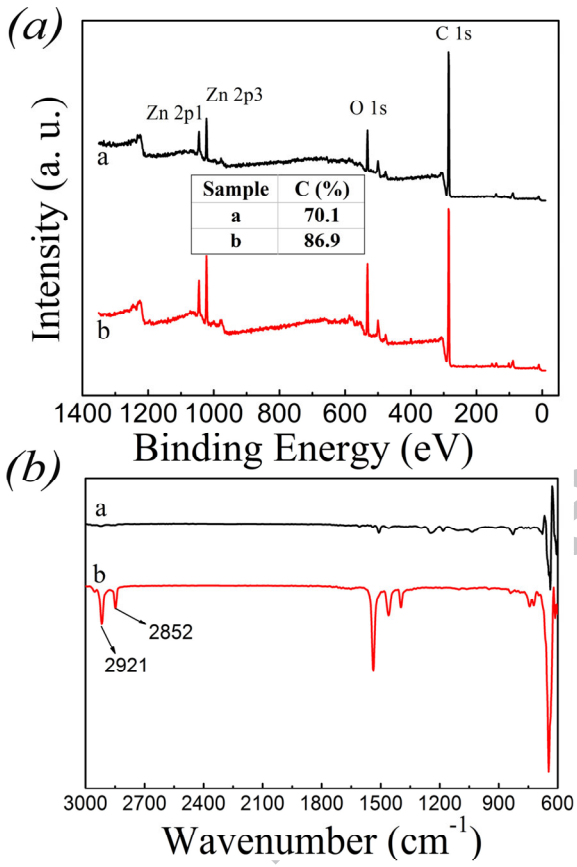

Fig. 3 XPS (a) and FTIR (b) spectra of the ZnO/ER coating (curve a), and the micro-nanoscale flowerlike ZnO/ER superhydrophobic coating (curve b).

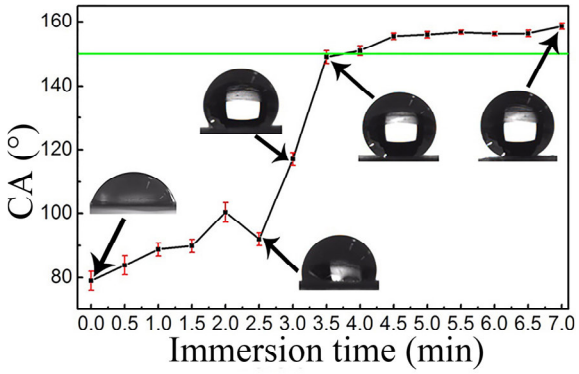

Fig. 4 CA and optical images of static water droplets (5 μL) of the ZnO/ER coating for different immersion time.

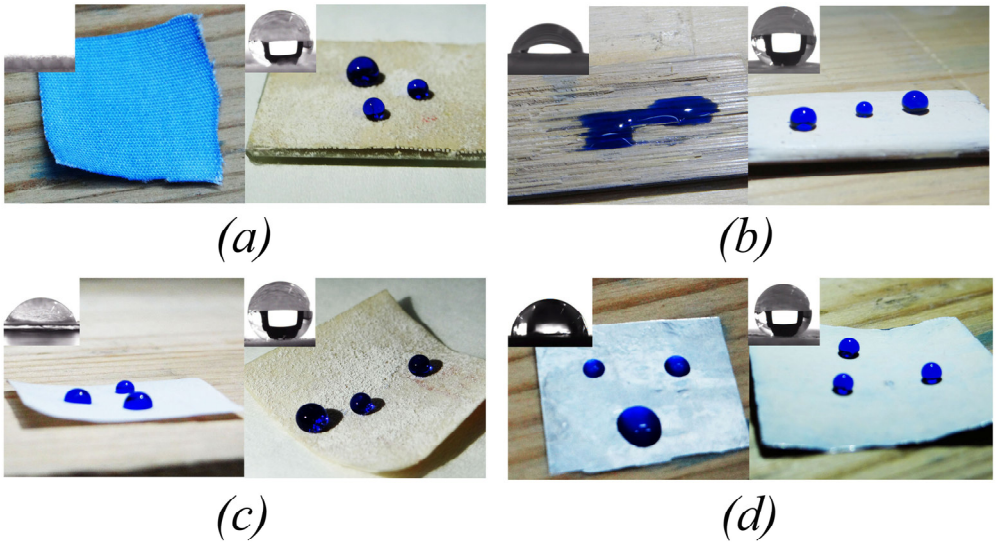

Fig. 5 Photographs of water droplets on the surfaces of fabric (a), wood (b), paper (c), and metal (d), before and after immersion. Shown in the insets are the optical images of the static water droplets (5 μL).

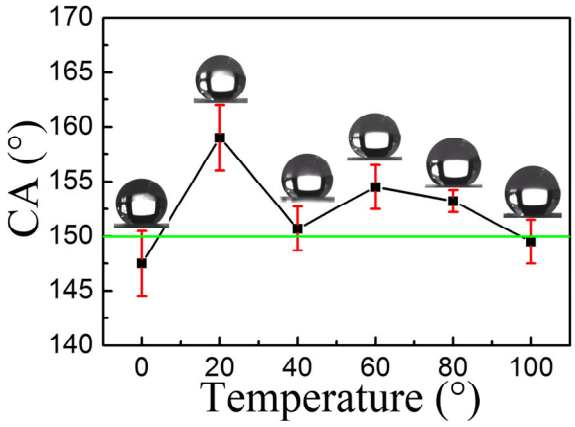

Fig. 6 CA and optical images of static water droplets (5 μL) of the micro-nanoscale flowerlike ZnO/ER superhydrophobic coating at different temperatures.

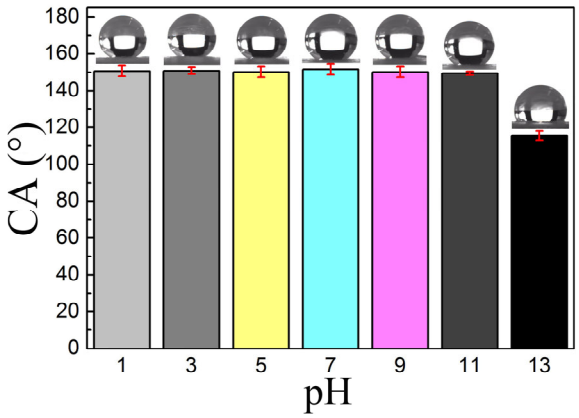

Fig. 7 CA and optical images of static water droplets (5 μL) of the micro-nanoscale flowerlike ZnO/ER superhydrophobic coating at different pH values.

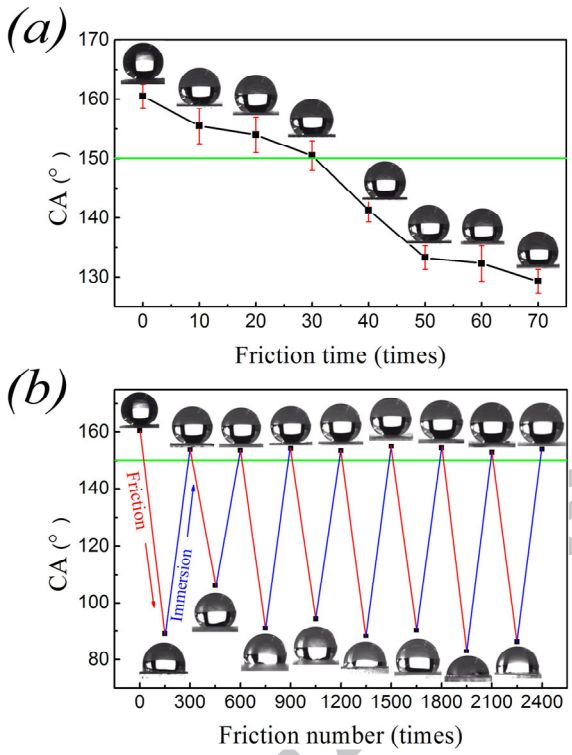

Fig. 8 (a) CA and optical images of static water droplets (5 μL) of the micro-nanoscale flowerlike ZnO/ER superhydrophobic coating after each friction cycle (10 times per cycle). (b) Reversible superhydrophobicity-superhydrophilicity switching of the micro-nanoscale flowerlike ZnO/ER superhydrophobic coating under friction (300 times per cycle) and immersion.

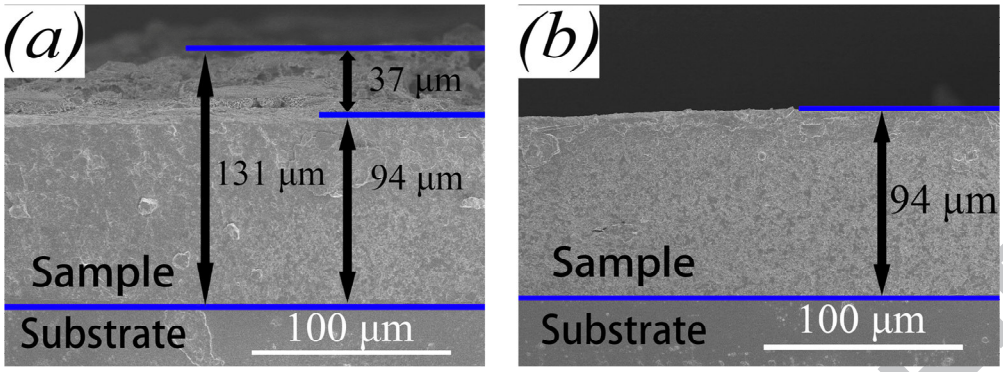

Fig. 9 Thickness of the micro-nanoscale flowerlike ZnO/ER superhydrophobic coating before (a) and after (b) 2400 friction times.

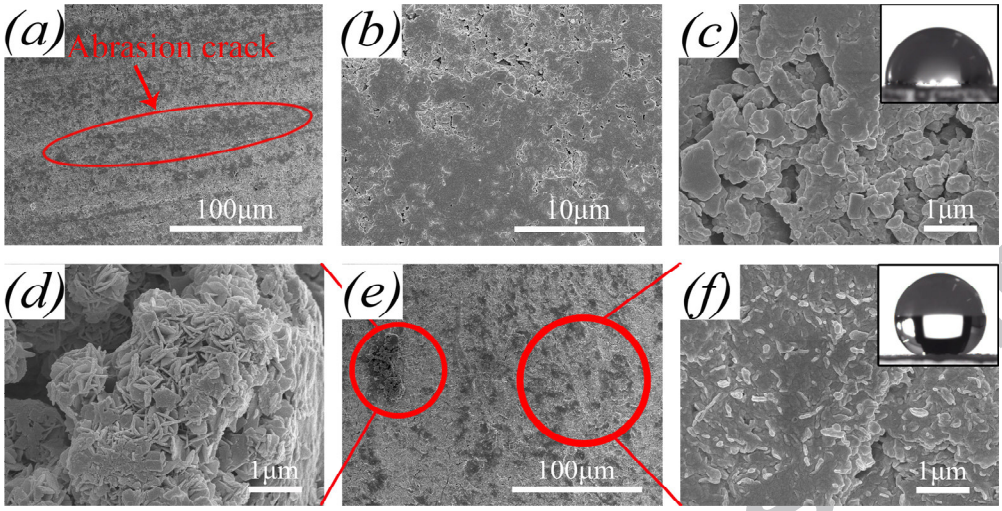

Fig. 10 Different magnification SEM images of the micro-nanoscale flowerlike ZnO/ER superhydrophobic coating after friction; (a), (b), and (c), and after immersion; (d), (e), and (f). Shown in the insets of (c) and (f) are the optical images of static water droplets (5 μL).

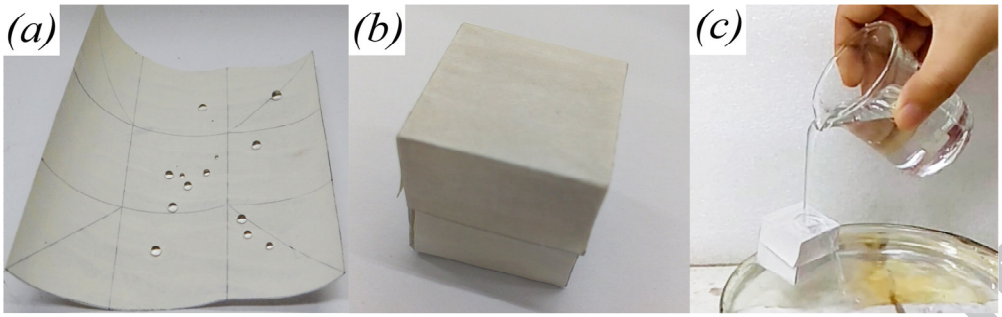

Fig. 11 (a) Superhydrophobic square paper with the micro-nanoscale flowerlike ZnO/ER superhydrophobic coating is used to make a superhydrophobic box. (b) The superhydrophobic paper box used in experiment was made using two superhydrophobic square papers. (c) Putting the box on the water surface and watering from above to simulate a wet environment on a rainy day for testing the superhydrophobicity of the box.

Table 1 Water CA of samples before and after immersion.

Sample	CA (°)	
	Before	after
Fabric	0	154
Wood	79.8	157
Paper	65.8	157
Metal	89.0	157

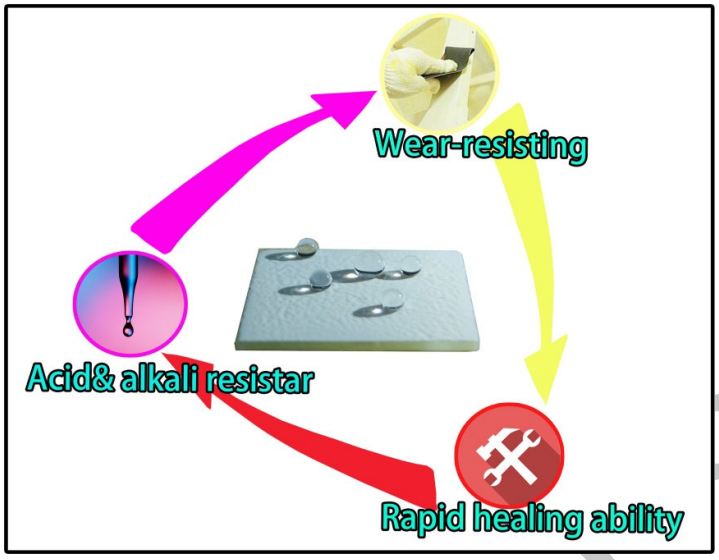

Robust micro-nanoscale flower-like ZnO @ epoxy resin superhydrophobic coating with excellent mechanical stability and chemical durability and can be large-scale prepared and keep its properties for a long time which can satisfies a completely need of our real life. And it has three protective abilities to cope with a variety of possible extreme nature environments.

Highlights

1. An immersion method was successfully used
2. The micro-nanoscale flower-like ZnO @ Epoxy resin superhydrophobic coating was fabricated
3. The coating shows superhydrophobic properties.
4. The coating can be easily repaired for many times.
5. The coating also has wide applications in real life for many substrates at 20 °C ~ 80 °C temperature